



Contents lists available at ScienceDirect

Chinese Chemical Letters

journal homepage: [www.elsevier.com/locate/cclet](http://www.elsevier.com/locate/cclet)



Communication

# An efficient Ag/MIL-100(Fe) catalyst for photothermal conversion of CO<sub>2</sub> at ambient temperature

Peng Jing<sup>a</sup>, Boyuan Wu<sup>a</sup>, Zongsu Han<sup>a</sup>, Wei Shi<sup>a,\*</sup>, Peng Cheng<sup>a,b</sup>

<sup>a</sup> Key Laboratory of Advanced Energy Materials Chemistry (MOE), College of Chemistry, Nankai University, Tianjin 300071, China

<sup>b</sup> Renewable Energy Conversion and Storage Center, Nankai University, Tianjin 300071, China

ARTICLE INFO

Article history:

Received 21 February 2021

Received in revised form 24 March 2021

Accepted 25 March 2021

Available online xxx

Keywords:

Ag nanoparticles

Metal-organic frameworks

Photothermal catalysis

CO<sub>2</sub> conversion

Carboxylation

ABSTRACT

The conversion of CO<sub>2</sub> under mild condition is of great importance because these reactions involving CO<sub>2</sub> can not only produce value-added chemicals from abundant and inexpensive CO<sub>2</sub> feedstock but also close the carbon cycle. However, the chemical inertness of CO<sub>2</sub> requires the development of high-performance catalysts. Herein, Ag nanoparticles/MIL-100(Fe) composites were synthesized by simple impregnation-reduction method and employed as catalysts for the photothermal carboxylation of terminal alkynes with CO<sub>2</sub>. MIL-100(Fe) could stabilize Ag nanoparticles and prevent them from aggregation during catalytic process. Taking the advantages of photothermal effects and catalytic activities of both Ag nanoparticles and MIL-100(Fe), various aromatic alkynes could be converted to corresponding carboxylic acid products (86%–92% yields) with 1 atm CO<sub>2</sub> at room temperature under visible light irradiation when using Ag nanoparticles/MIL-100(Fe) as photothermal catalysts. The catalysts also showed good recyclability with almost no loss of catalytic activity for three consecutive runs. More importantly, the catalytic performance of Ag nanoparticles/MIL-100(Fe) under visible light irradiation at room temperature was comparable to that upon heating, showing that the light source could replace conventional heating method to drive the reaction. This work provided a promising strategy of utilizing solar energy for achieving efficient CO<sub>2</sub> conversion to value-added chemicals under mild condition.

© 2021 Chinese Chemical Society and Institute of Materia Medica, Chinese Academy of Medical Sciences.

Published by Elsevier B.V. All rights reserved.

The increasing demand for energy has led to the consumption of large quantities of fossil fuels, which in turn causes increased anthropogenic CO<sub>2</sub> emission. This excess production of CO<sub>2</sub> is credited with causing adverse impact on climate such as global warming [1]. Therefore, reduction of CO<sub>2</sub> concentration while maintaining fossil fuel energy supply at present is crucial from both technological and environmental perspectives. In contrast to CO<sub>2</sub> storage, transformation of CO<sub>2</sub> to value-added chemicals is more attractive since it can offer higher efficiency of energy conversion and storage [2]. Among various reactions involving CO<sub>2</sub>, the synthesis of carboxylic acids and their derivatives attracts much attention because high value-added carboxylic acids are important products or intermediates in medical chemistry (e.g., aspirin) and organic synthesis [3–9]. The global market value associated with carboxylic acids will possibly increase to €16 billion by 2024 [10]. Although there are diverse protocols for the preparation of carboxylic acids such as carbonylation of organic halides with toxic carbon monoxide, the one-step carboxylation of

carbon nucleophiles using abundant and inexpensive CO<sub>2</sub> as C1 electrophile is the simplest and the most straightforward method. Although the efficient carboxylation of C–H bond with CO<sub>2</sub> under green and mild conditions have been achieved [11–15], limited by the thermodynamic stability and kinetic inertness of CO<sub>2</sub>, the carboxylation of terminal alkynes with CO<sub>2</sub> were usually performed at elevated temperatures or under high CO<sub>2</sub> pressures which cause additional environmental issues [16–18]. Therefore, the development of efficient catalysts that can catalyze the reaction under mild condition is highly desirable.

The utilization of solar energy as a renewable energy source can not only meet the increasing global energy demand but also offer a solution to the growing environmental concerns of greenhouse gases. By making use of the photothermal effect, light source can be employed to replace conventional heating method to drive the reaction, realizing the storage and transformation of solar energy with high efficiency [19,20]. Ag nanoparticles (NPs) are promising photothermal materials because they have strong surface plasmon resonance (SPR) effects that can induce temperature increase of the surrounding environment under light irradiation [21,22]. Ag NPs are also active for the conversion of CO<sub>2</sub> [18]. However, they tend to aggregate during catalytic process and are difficult to

\* Corresponding author.

E-mail address: [shiwei@nankai.edu.cn](mailto:shiwei@nankai.edu.cn) (W. Shi).

<https://doi.org/10.1016/j.ccllet.2021.04.007>

1001-8417/© 2021 Chinese Chemical Society and Institute of Materia Medica, Chinese Academy of Medical Sciences. Published by Elsevier B.V. All rights reserved.

recover to small nanoparticles and hence require porous materials as matrix to keep their uniform dispersion. As a kind of porous crystalline materials with high surface areas, metal-organic frameworks (MOFs) cannot only stabilize surface-clean NPs by spatial confinement, but also provide abundant catalytically active sites for CO<sub>2</sub> conversion [23–29]. Moreover, MOFs were found to exhibit photothermal effects [30–32]. To date, metal NPs-MOF composites have been exploited in photothermal therapy and catalytic reactions such as hydrogenation of olefins [33–36].

In photothermal CO<sub>2</sub>-involved catalytic reactions, on one hand, photothermal hydrogenation of CO<sub>2</sub> to obtain different chemicals like CO, HCOOH, CH<sub>3</sub>OH or CH<sub>4</sub> have been achieved using transition metal-based catalysts [37–42]. On the other hand, it is still of great significance to develop other strategies for photothermal CO<sub>2</sub> conversion, such as photothermal CO<sub>2</sub>-involved organic synthesis. Herein, a series of Ag NPs/MIL-100(Fe) with different Ag loadings were synthesized and their catalytic performance toward carboxylation of terminal alkynes with 1 atm CO<sub>2</sub> under visible light irradiation at room temperature were evaluated. Owing to the synergistic effect of Ag NPs and MIL-100(Fe), their catalytic performance without direct heating was comparable to that heated at 50 °C.

MIL-100(Fe), a well-known MOF with high stability and porosity, was chosen as not only the support for Ag NPs but also the catalyst with abundant Lewis acid active sites [43,44]. An impregnation-reduction method was introduced to load Ag NPs on MIL-100(Fe) (Scheme 1). MIL-100(Fe) was impregnated in the acetonitrile solution of AgNO<sub>3</sub> to adsorb Ag ions on its surface. The solvent was totally removed by vacuumizing, and the residue with adsorbed Ag ions was reduced by NaBH<sub>4</sub> to obtain Ag/MIL-100(Fe). The concentration of AgNO<sub>3</sub> was varied to prepare Ag/MIL-100(Fe) with different Ag loadings: 5 wt%, 10 wt%, 15 wt% and 20 wt%, which were denoted herein as 5Ag/MIL-100(Fe), 10Ag/MIL-100(Fe), 15Ag/MIL-100(Fe) and 20Ag/MIL-100(Fe) respectively. The actual Ag loadings were determined by inductively coupled plasma atomic emission spectroscopy (ICP-AES) as shown in Table S1 in Supporting information, which were close to the expected loadings. The relatively low Ag loading of 16.4 wt% in 20Ag/MIL-100(Fe) was due to the loss of larger Ag NPs that could not be immobilized stably by MIL-100(Fe) during washing step.

Powder X-ray diffraction (PXRD) patterns of the prepared composites confirmed their high crystallinity (Fig. 1). Weak diffraction peaks at 38.12° were attributed to Ag NPs (JCPDS No. 04-0783) and their intensities increased with increasing Ag loadings. The Brunauer-Emmett-Teller (BET) surface areas of these composites were analyzed by N<sub>2</sub> adsorption-desorption isotherms at 77 K (Fig. 2). Although the BET surface areas decreased slightly after loading Ag NPs (Table S1), the potential catalytically active sites of MIL-100(Fe) were still accessible to the guests.

UV-vis absorption spectra of MIL-100(Fe) and Ag/MIL-100(Fe) were measured to investigate their light absorption properties. MIL-100(Fe) exhibited absorption centred at 320 and 445 nm (Fig. 3) due to ligand-to-metal charge transfer and d-d transition of

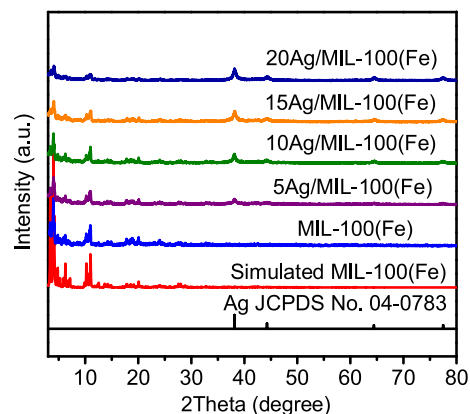


Fig. 1. PXRD patterns of MIL-100(Fe) and Ag/MIL-100(Fe) with different Ag loadings.

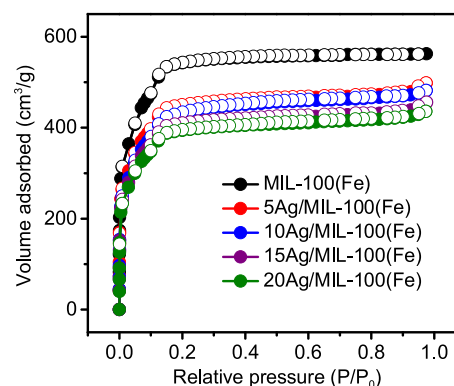


Fig. 2. N<sub>2</sub> adsorption-desorption isotherms (77 K) of MIL-100(Fe) and Ag/MIL-100(Fe) with different Ag loadings.

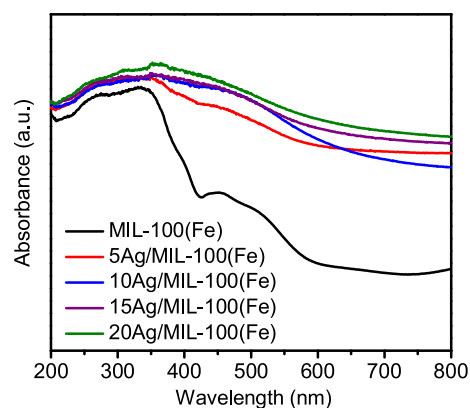
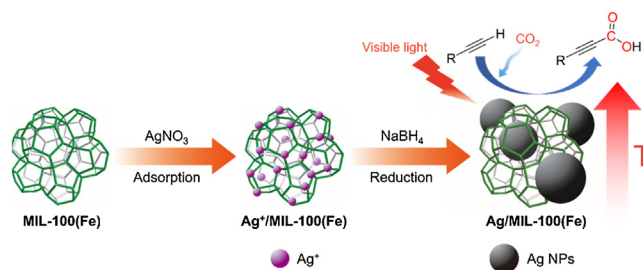


Fig. 3. UV-vis absorption spectra of MIL-100(Fe) and Ag/MIL-100(Fe) with different Ag loadings.



Scheme 1. Synthetic route to Ag/MIL-100(Fe) and photothermal conversion of CO<sub>2</sub>.

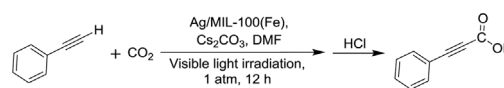
metal nodes [45–48]. After loading Ag NPs, enhanced absorption of Ag/MIL-100(Fe) in the visible region was originated from SPR effects of Ag NPs [45,49–51], which indicated high harvesting efficiency of light energy by Ag/MIL-100(Fe). To investigate the photothermal effects of Ag/MIL-100(Fe), the temperature increases of the solutions caused by MIL-100(Fe) and Ag/MIL-100(Fe) under visible light irradiation (accounts for 43% of solar energy) after 0.5 h were measured (Table S2 in Supporting information). For pristine MIL-100(Fe), the temperature increased by 17 °C. After loading Ag NPs on MIL-100(Fe), higher temperature increases of

18–26 °C were observed, which were consistent with their light absorption properties. The results also revealed that both Ag NPs and MIL-100(Fe) contributed to increased temperature of the solution. For comparison, when activated carbon (AC) was used as support, 15Ag/AC showed more prominent photothermal effect with a temperature increase of 27 °C due to the broad absorption of both Ag NPs and AC in visible region (Fig. S1 in Supporting information).

Transmission electron microscopy (TEM) images showed that Ag NPs with diameters of 5–7 nm were uniformly distributed on MIL-100(Fe) (Fig. 4a and Fig. S2 in Supporting information). Ag NPs with diameters > 9 nm were also formed when Ag loading was increased to 15 wt%. The diameters of most Ag NPs were larger than the pore sizes (2.5 and 2.9 nm) of MIL-100(Fe), indicating that Ag NPs were located on the surface and/or encapsulated in the framework of MIL-100(Fe) which could prevent the growth of Ag NPs [52]. Scanning electron microscopy (SEM) images and energy-dispersive X-ray spectroscopy (EDS) elemental mapping results also confirmed the uniform distributions of Ag NPs on MIL-100(Fe) (Figs. 4b–e and Figs. S3–S5 in Supporting information). For comparison, only large Ag NPs (> 15 nm) were obtained for 15Ag/AC (Fig. S6 in Supporting information).

Encouraged by the photothermal effect of Ag/MIL-100(Fe), their catalytic activities toward photothermal carboxylation of terminal alkynes with CO<sub>2</sub> were evaluated. 1-ethynylbenzene was employed as model substrate. The reactions were performed under 1 atm CO<sub>2</sub> and visible light irradiation (420 nm < λ < 780 nm) at room temperature for 12 h and the corresponding yields of 3-phenylpropionic acid were presented in Table 1. MIL-100(Fe) afforded the yield of 47% due to its accessible Lewis acid active sites [53]. When Ag NPs were loaded, Ag/MIL-100(Fe) exhibited better catalytic performance than MIL-100(Fe), proving that the SPR effect of Ag NPs was able to promote the carboxylation reaction. The yields increased from 69% to 92% as the Ag loadings increased from 5 wt% to 15 wt%. 3-Phenylpropionic acid was formed with the highest yield of 92% for optimal 15Ag/MIL-100(Fe). However, a decreased yield of 83% could be observed when further increasing Ag loading to 20 wt% because large Ag NPs exhibited inferior catalytic activities than small Ag NPs. There were works of the carboxylation of terminal alkynes with CO<sub>2</sub> using various catalysts including Ag/MIL-100(Fe) with good yields (> 90%) obtained (Table S3 in Supporting information). However, most of them were performed under heating conditions. Although several reactions could proceed at room temperature, prolonged reaction times were required. In this work, the yield of above 90% could be achieved without heating in less reaction time (12 h). The possible reaction mechanism had been proposed (Fig. S7 in Supporting information)

**Table 1**  
Synthesis of 3-phenylpropionic acid from CO<sub>2</sub> and 1-ethynylbenzene.<sup>a</sup>



Entry	Catalyst	Time (h)	Yield (%) <sup>b</sup>
1	MIL-100(Fe)	12	47
2	5Ag/MIL-100(Fe)	12	69
3	10Ag/MIL-100(Fe)	12	79
4	15Ag/MIL-100(Fe)	6	62
5	15Ag/MIL-100(Fe)	12	92
6	20Ag/MIL-100(Fe)	12	83
7	15Ag/AC	12	39
8 <sup>c</sup>	15Ag/MIL-100(Fe)	12	91
9 <sup>d</sup>	15Ag/MIL-100(Fe)	12	54
10 <sup>e</sup>	15Ag/MIL-100(Fe)	12	75

<sup>a</sup> Reaction conditions: catalyst (30 mg), 1-ethynylbenzene (0.5 mmol), Cs<sub>2</sub>CO<sub>3</sub> (0.6 mmol), CO<sub>2</sub> (1 atm), DMF (5 mL), visible light irradiation, room temperature.

<sup>b</sup> Isolated yield.

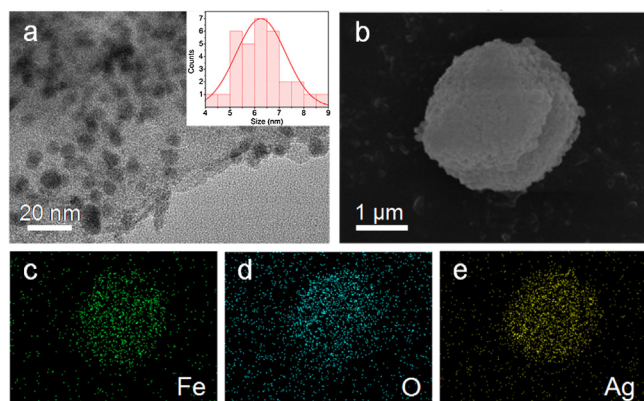
<sup>c</sup> Replacing light with heating at 50 °C.

<sup>d</sup> Room temperature without light.

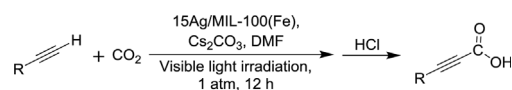
<sup>e</sup> Simulated sunlight.

[18]. The alkyne was activated by Ag NPs and Lewis acid active sites in MIL-100(Fe) and deprotonated by Cs<sub>2</sub>CO<sub>3</sub> to form the metal acetylide. Then the insertion of CO<sub>2</sub> into the carbon-metal bonds afforded metal propiolate intermediate. Finally, metal propiolate intermediate reacted with another terminal alkyne and Cs<sub>2</sub>CO<sub>3</sub> to form cesium propiolate and regenerated metal acetylide for next cycle. The carboxylic acid product could be obtained by acidification of cesium propiolate.

To further demonstrate the synergistic effect of Ag NPs and MIL-100(Fe) on enhanced catalytic performance, the reaction was carried out with 15Ag/AC as catalyst. Although 15Ag/AC showed strong photothermal effect, the diameters of Ag NPs in 15Ag/AC were much larger than those in Ag/MIL-100(Fe) and the AC structure did not contain catalytically active sites. As a result, the yield of 3-phenylpropionic acid for 15Ag/AC was only 39%. This result revealed that not only the photothermal effects but also the catalytic activities of both Ag NPs and MIL-100(Fe) were important in improving catalytic efficiency. For comparison, the reaction was also performed under the same condition with light irradiation replaced by heating (50 °C). The corresponding yield of 91% was similar to that achieved under visible light irradiation (Table 1, entry 8). This result confirmed that the carboxylation of 1-ethynylbenzene with 1 atm CO<sub>2</sub> could be achieved effectively using visible light irradiation as an alternative to energy-consuming heating when 15Ag/MIL-100(Fe) served as the catalyst. The reactions under room temperature (without light) and simulated sunlight by using AM1.5 filter were also performed and corresponding yields were 54% and 75% (Table 1, entries 9 and 10). The results showed that although the reaction could proceed at room temperature, an elevated temperature was required to achieve high product yield. In addition, the lower light intensity (100 mW/cm<sup>2</sup>) of simulated sunlight compared with that (200 mW/cm<sup>2</sup>) of pre-set visible light led to lower temperature increase (16 °C), and thus gave inferior performance. Furthermore, the carboxylation of other aromatic alkynes with electron-withdrawing (Cl) or electron-donating (CH<sub>3</sub>, OCH<sub>3</sub>) moieties were also investigated (Table 2). The reaction of electron-withdrawing moiety substituted aromatic alkyne exhibited 90% yield and the aromatic alkynes with electron-donating moieties could be converted to corresponding products with the yields of 87%–88%. 86% yield could also be achieved for alkyne with a heterocyclic group. Moreover, the recycling test showed that the yield could be maintained above 80% after three cycles (Fig. 5a). The decreased yield was probably due to the partial



**Fig. 4.** (a) TEM image, (b–e) SEM image and corresponding elemental mappings of 15Ag/MIL-100(Fe). Inset in (a) was size distribution of Ag NPs.

**Table 2**  
Synthesis of propiolic acid derivatives from CO<sub>2</sub> and alkynes.<sup>a</sup>

Entry	Alkyne	Product	Yield (%) <sup>b</sup>
1			92
2			90
3			87
4			88
5			86

<sup>a</sup> Reaction conditions: 15Ag/MIL-100(Fe) (30 mg), alkynes (0.5 mmol), Cs<sub>2</sub>CO<sub>3</sub> (0.6 mmol), CO<sub>2</sub> (1 atm), DMF (5 mL), visible light irradiation, room temperature.

<sup>b</sup> Isolated yield.

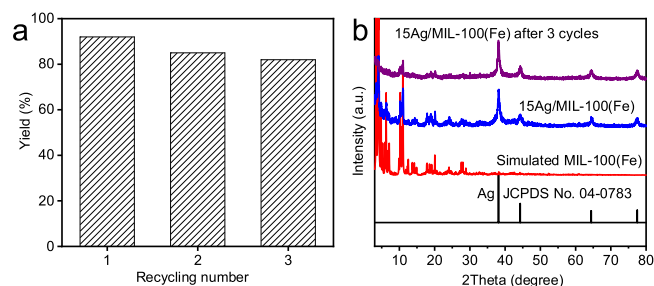


**Fig. 5.** (a) Catalytic recycling test of carboxylation of 1-ethynylbenzene with CO<sub>2</sub> using 15Ag/MIL-100(Fe) catalyst. (b) PXRD pattern of 15Ag/MIL-100(Fe) after 3 cycles.

decomposition of MIL-100(Fe) in alkaline solution which could be confirmed by decreased peak intensities of MIL-100(Fe) in PXRD pattern (Fig. 5b).

In summary, Ag/MIL-100(Fe) composites were prepared using MIL-100(Fe) as support through a facile solution impregnation-reduction method. The framework structure of MIL-100(Fe) stabilized Ag NPs and prevented their aggregation during the catalytic process. Both MIL-100(Fe) and Ag NPs exhibited photothermal effects and catalytic activities for carboxylation of terminal alkynes with CO<sub>2</sub>. Remarkably, benefiting from the synergistic effects of Ag NPs and MIL-100(Fe), Ag/MIL-100(Fe) catalyst could efficiently promote carboxylation of terminal alkynes with 1 atm CO<sub>2</sub> under visible light irradiation at room temperature and the yield was comparable to that obtained by heating. This work demonstrated an efficient strategy for catalyzing photothermal organic reaction with CO<sub>2</sub>, and provided a promising approach of utilizing solar energy to drive CO<sub>2</sub> conversion in the future.

#### Declaration of competing interest

The authors report no declarations of interest.

#### Acknowledgments

This work was supported by the Natural Science Foundation of Tianjin (No. 18JCJQC47200), the Ministry of Education of China (No. B12015) and the Fundamental Research Funds for the Central Universities, Nankai University (Nos. 63201016 and 63201043).

#### Appendix A. Supplementary data

Supplementary material related to this article can be found, in the online version, at doi:<https://doi.org/10.1016/j.cclet.2021.04.007>.

#### References

- [1] A. Goepfert, M. Czaun, J.P. Jones, G.K. Surya Prakash, G.A. Olah, Chem. Soc. Rev. 43 (2014) 7995–8048.
- [2] D.P. Schrag, Science 315 (2007) 812–813.
- [3] E.V. Kondratenko, G. Mul, J. Baltrusaitis, G.O. Larrazábal, J. Pérez-Ramírez, Energy Environ. Sci. 6 (2013) 3112–3135.
- [4] X.B. Lu, D.J. Darensbourg, Chem. Soc. Rev. 41 (2012) 1462–1484.
- [5] Q. Liu, L. Wu, R. Jackstell, M. Beller, Nat. Commun. 6 (2015) 5933.
- [6] J. Liu, C. Chen, K. Zhang, L. Zhang, Chin. Chem. Lett. (2020), doi:<http://dx.doi.org/10.1016/j.cclet.2020.07.040>.
- [7] M. Aresta, A. Dibenedetto, A. Angelini, Chem. Rev. 114 (2014) 1709–1742.
- [8] Q.W. Song, Z.H. Zhou, L.N. He, Green Chem. 19 (2017) 3707–3728.
- [9] D. Yu, S.P. Teong, Y. Zhang, Coord. Chem. Rev. 293–294 (2015) 279–291.
- [10] R. Martin, A. Tortajada, F. Juliá-Hernández, M. Borjesson, T. Moragas, Angew. Chem. Int. Ed. 57 (2018) 15948–159820.
- [11] I.I.F. Boogaerts, S.P. Nolan, J. Am. Chem. Soc. 132 (2010) 8858–8859.
- [12] Q.Y. Meng, T.E. Schirmer, A.L. Berger, K. Donabauer, B. König, J. Am. Chem. Soc. 141 (2019) 11393–11397.
- [13] C.S. Yeung, Angew. Chem. Int. Ed. 58 (2019) 5491–5502.
- [14] M. Borjesson, D. Janssen-Muller, B. Sahoo, et al., J. Am. Chem. Soc. 142 (2020) 16234–16239.
- [15] L. Song, D.M. Fu, L. Chen, et al., Angew. Chem. Int. Ed. 59 (2020) 21121–21128.
- [16] B. Yu, J.N. Xie, C.L. Zhong, W. Li, L.N. He, ACS Catal. 5 (2015) 3940–3944.
- [17] P. Bhanja, A. Modak, A. Bhaumik, Chem. Eur. J. 24 (2018) 7278–7297.
- [18] X.H. Liu, J.G. Ma, Z. Niu, G.M. Yang, P. Cheng, Angew. Chem. Int. Ed. 54 (2015) 988–991.
- [19] S. Wu, Y. Li, Q. Zhang, et al., Adv. Energy Mater. 10 (2020) 2002602.
- [20] Y. Li, L. Wang, J. Low, et al., Chin. Chem. Lett. 31 (2020) 231–234.
- [21] L.M. Liz-Marzan, C.J. Murphy, J. Wang, Chem. Soc. Rev. 43 (2014) 3820–3822.
- [22] S. Linic, U. Aslam, C. Boerigter, M. Morabito, Nat. Mater. 14 (2015) 567–576.
- [23] J. Lee, O.K. Farha, J. Roberts, et al., Chem. Soc. Rev. 38 (2009) 1450–1459.
- [24] H.C. Zhou, J.R. Long, O.M. Yaghi, Chem. Rev. 112 (2012) 673–674.
- [25] Q. Yang, Q. Xu, H.L. Jiang, Chem. Soc. Rev. 46 (2017) 4774–4808.
- [26] R. Mahugo, A. Mayor, M. Sánchez-Sánchez, I. Diaz, Front. Chem. 7 (2019) 686.
- [27] M. Ding, R.W. Flaig, H.L. Jiang, O.M. Yaghi, Chem. Soc. Rev. 48 (2019) 2783–2828.
- [28] G. Cai, M. Ding, Q. Wu, H.L. Jiang, Natl. Sci. Rev. 7 (2019) 37–45.
- [29] Y. Pan, Y. Qian, X. Zheng, et al., Natl. Sci. Rev. 8 (2021) nwaa224.
- [30] J. Espín, L. Garzón-Tovar, G. Boix, I. Imaz, D. Maspoch, Chem. Commun. 54 (2018) 4184–4187.
- [31] J. Espín, L. Garzón-Tovar, A. Carné-Sánchez, I. Imaz, D. Maspoch, ACS Appl. Mater. Interfaces 10 (2018) 9555–9562.
- [32] J.D. Xiao, H.L. Jiang, Acc. Chem. Res. 52 (2019) 356–366.
- [33] K. Khaletskaya, J. Reboul, M. Meilikhov, et al., J. Am. Chem. Soc. 135 (2013) 10998–11005.
- [34] X. Liu, L. He, J. Zheng, et al., Adv. Mater. 27 (2015) 3273–3277.
- [35] Q. Yang, Q. Xu, S.H. Yu, H.L. Jiang, Angew. Chem. Int. Ed. 55 (2016) 3685–3689.
- [36] F. Wang, Y. Huang, Z. Chai, et al., Chem. Sci. 7 (2016) 6887–6893.
- [37] X. Meng, T. Wang, L. Liu, et al., Angew. Chem. Int. Ed. 53 (2014) 11478–11482.
- [38] W. Zhang, L. Wang, K. Wang, et al., Small 13 (2017) 1602583.
- [39] G. Chen, R. Gao, Y. Zhao, et al., Adv. Mater. 30 (2018) 1704663.
- [40] A.A. Jelle, K.K. Ghuman, P.G. O'Brien, et al., Adv. Energy Mater. 8 (2018) 1702277.
- [41] Q. Yang, C.C. Yang, C.H. Lin, H.L. Jiang, Angew. Chem. Int. Ed. 58 (2019) 3511–3515.
- [42] Q. Guo, S.G. Xia, X.B. Li, et al., Chem. Commun. 56 (2020) 7849–7852.
- [43] M. Opanasenko, A. Dhakshinamoorthy, Y.K. Hwang, et al., ChemSusChem 6 (2013) 865–871.
- [44] J. Kim, S.N. Kim, H.G. Jang, G. Seo, W.S. Ahn, Appl. Catal. A 453 (2013) 175–180.
- [45] R. Liang, S. Luo, F. Jing, et al., Appl. Catal. B 176–177 (2015) 240–248.
- [46] K.G.M. Laurier, F. Vermoortele, R. Ameloot, et al., J. Am. Chem. Soc. 135 (2013) 14488–14491.
- [47] A. Dhakshinamoorthy, A.M. Asiri, H. García, Angew. Chem. Int. Ed. 55 (2016) 5414–5445.
- [48] L. Zhu, M. Gao, C.K.N. Peh, G.W. Ho, Mater. Horiz. 5 (2018) 323–343.
- [49] Y. Sun, Y. Yin, B.T. Mayers, T. Herricks, Y. Xia, Chem. Mater. 14 (2002) 4736–4745.
- [50] K.L. Kelly, E. Coronado, L.L. Zhao, G.C. Schatz, J. Phys. Chem. B 107 (2003) 668–677.
- [51] X. Meng, L. Liu, S. Ouyang, et al., Adv. Mater. 28 (2016) 6781–6803.
- [52] H.L. Jiang, T. Akita, T. Ishida, M. Haruta, Q. Xu, J. Am. Chem. Soc. 133 (2011) 1304–1306.
- [53] P.L. Llewellyn, S. Bourrelly, C. Serre, et al., Langmuir 24 (2008) 7245–7250. doi:10.1021/la72457250.